3nd European supercritical CO2 Conference
September 19-20, 2019, Paris, France

2019-sCO2.eu-155

TRANSIENT RESPONSE OF SUPERCRITICAL CO_2 AXIAL TURBINE FOR KAIST MMR

In-woo Son
[a] *Department of Nuclear and Quantum Engineering, Korea Advanced Institute of Science and Technology 373-1 Guseong-dong Yuseong-gu, Daejeon, 305-701, Korea*
Email: siw4139@kaist.ac.kr

Jin Young Heo
[a] *Department of Nuclear and Quantum Engineering, Korea Advanced Institute of Science and Technology 373-1 Guseong-dong Yuseong-gu, Daejeon, 305-701, Korea*
Email: jyh9090@kaist.ac.kr

Bong Seong Oh
[a] *Department of Nuclear and Quantum Engineering, Korea Advanced Institute of Science and Technology 373-1 Guseong-dong Yuseong-gu, Daejeon, 305-701, Korea*
Email: bongseongoh@kaist.ac.kr

Jeong Ik Lee
[a] *Department of Nuclear and Quantum Engineering, Korea Advanced Institute of Science and Technology 373-1 Guseong-dong Yuseong-gu, Daejeon, 305-701, Korea*
mail: jeongiklee@kaist.ac.kr

ABSTRACT

The Supercritical CO_2 (S-CO_2) Brayton power cycle has the advantages of relatively high efficiency at moderate heat source temperature compared to a steam Rankine cycle or a helium Brayton cycle and compact components size. In nuclear energy industry, Small Modular Reactors have potentials in many aspects, flexibility of construction, and applicability for the distributed power source and reduced construction cost. Therefore, KAIST research team developed an S-CO_2 cooled Small Modular Reactor namely KAIST Micro Modular Reactor (MMR), using both advantages of S-CO_2 cycle and SMR. Currently, radial turbine is being used for the output of 12MWe in MMR. The original KAIST-MMR was designed to utilize radial turbine but the 12MWe power output of MMR can adopt axial turbine as well. Therefore, this paper explores the potential of improving both steady state performance and transient response by switching from radial type to axial type turbine. The implications of the transient analysis results show the advantages of using the axial turbine over the radial turbine because the axial turbine operates at relatively higher efficiencies for wider off-design ranges.

INTRODUCTION

The supercritical CO_2 (S-CO_2) cycle is attracting attention as it has the potential to replace the existing steam cycle in the process of developing the next generation nuclear power plants. In addition, the supercritical CO_2 cycle has a higher thermal efficiency than the steam Rankine cycle and the helium Brayton cycle when the turbine inlet temperature is above 500 degree Celsius [1, 2]. It also has the advantage that the components of the cycle, such as turbines and compressors, are more compact than other cycles, making them well suited for small modular nuclear reactors. Fig. 1 compares the efficiency of a supercritical CO_2 Brayton cycle, a steam Rankine cycle, and a helium Brayton cycle [1].

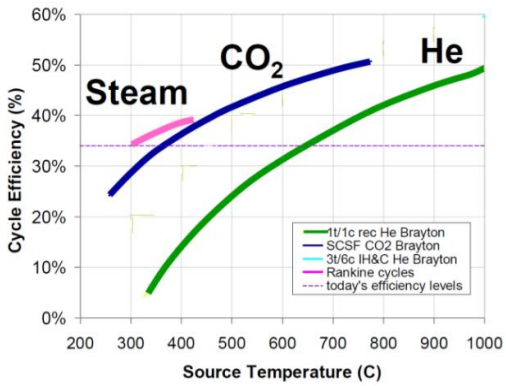

Fig. 1. Comparison of efficiency of S-CO_2 power cycle [1]

Recently, small modular reactor (SMR) technology has received worldwide attention, especially in developing countries. This is because it has the advantage in a region where power grid size is not large and distributed power generation can be more economical than the central power generation and distribution.

Based on these aspects, the KAIST research team developed a micro modular reactor (MMR) by combining two technologies:

 DOI: 10.17185/duepublico/48896

SMR and gas turbine technologies [3]. MMR is sized such that it can be transported via truck and the layout of MMR is shown in Fig. 2. The design values of MMR are summarized in Table 1. These values were obtained from the design process of a nuclear system by using validated in-house codes. The design was conducted by using the following well-validated programs: KAIST-TMD [5] and KAIST-HXD [6].

The KAIST TMD code for the compressor was validated in the previous study [5]. In addition, for the same turbomachinery, equivalent conditions can provide a basis for comparing different working fluids [7]. Furthermore, sCO_2 turbine operates where the properties are behaving similar to an ideal gas. Therefore, the KAIST TMD code was validated using NASA's air radial turbine data, which is equivalent to sCO_2 conditions for a radial turbine case [8]. For the axial turbine, the loss set of the following reference was used [9]. In ref. [9], the author selected the GTHTR 300 design of JAEA [10], a direct cycle using helium gas, as a reference model to validate the axial turbine code. Thus, KAIST-TMD is validated in radial compressor, radial turbine, and axial turbine with the available data.

The KAIST-HXD code was developed by the KAIST research team using a new thermal hydraulic correlation for sCO_2 heat exchanger and the code is validated by a laboratory-scale PCHE test at the KAIST supercritical CO_2 pressurizing experiment (SCO2PE) facility [6].

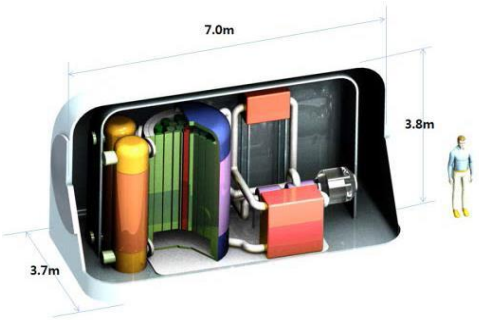

Fig. 2. Concept of KAIST-MMR [3]

Table 1. Summary of design results of MMR

Thermal power	36.2MWth	Net electric power	12MWe
Thermal efficiency	34.09%	Mechanical efficiency	98%
Mass flow rate	180.0kg/s	Total-to-total Pressure ratio	2.49
Turbine total-to-total efficiency	92%	Compressor total to total efficiency	85%
Generator efficiency	98%	Rotating speed	19,300rpm
Recuperator effectiveness	95%	Compressor inlet pressure	8.0MPa
Design point of recuperator	Hot side inlet : 440.7°C, 8.2MPa Cold side inlet : 142.1°C, 20.0MPa Temperature difference : 22-58°C		

DESCRIPTION OF KAIST-CCD, TMD, HXD CODE

KAIST-CCD

The KAIST-Closed Cycle Design (KAIST-CCD) code is based on MATLAB, and it is an in-house code developed by KAIST research team. Fig. 3 shows the main algorithm of the KAIST-CCD code. The monitored error value for the iteration is defined below.

$$Error = \frac{[heat\ input(n) - heat\ input(n-1)]}{heat\ input(n)} \qquad (1)$$

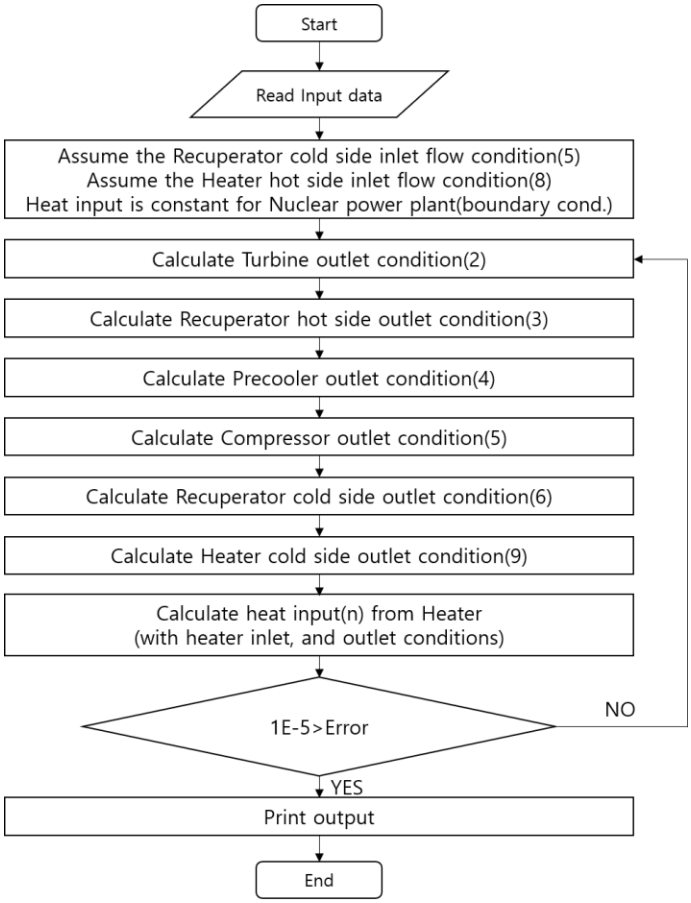

Fig. 3. Main algorithm of KAIST-CCD code for simple recuperated Brayton cycle [4].

Values of material properties such as enthalpy and entropy used in the code are provided by NIST-REFPROP (transport properties database) [11]. To illustrate how KAIST-CCD code works, the algorithm for the simple recuperated Brayton cycle analysis is shown in Fig. 3. The numbers in algorithm in Fig. 3 refer to the node numbers in Fig 4. First, read input data: fluid type, cycle layout, Total heat received by the cycle, max, min temperature of the cycle, max pressure of the cycle, efficiency, flow split and pressure ratio of the components. Second, the

 DOI: 10.17185/duepublico/48896

recuperator cold side inlet flow condition and the heater hot side inlet flow conditions are assumed. Next, the inlet and outlet conditions of each component are obtained using the models of the components and the assumed values. Finally, the heat input is obtained from the calculated condition values.

Since the heat source is prescribed, the error is estimated by comparing the prescribed heat source value to the calculated value. If the error is greater than or equal to 1E-5, the assumed values are updated to the calculated values.

Fig. 4 shows the nodes of the KAIST MMR for the KAIST CCD code. KAIST MMR is a system with a simple recuperated cycle as a power cycle and the shaft connects compressor and turbine to rotate at the same RPM. The CCD code is used to calculate the temperature, pressure, enthalpy, and entropy of each node. Therefore, the original MMR was optimized using KAIST-CCD when the turbine efficiency was changed.

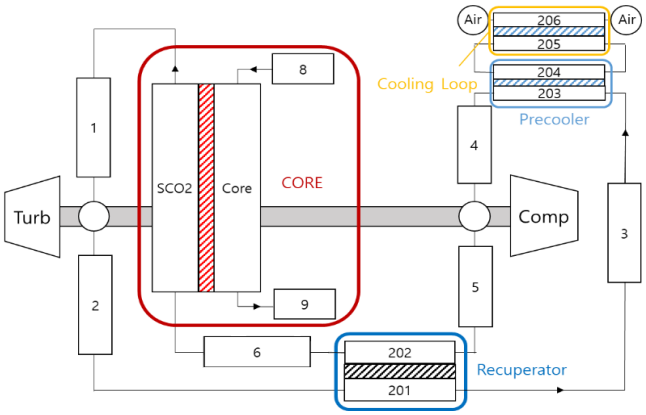

Fig. 4. Nodalization of MMR for CCD code

KAIST-TMD

The KAIST TurboMachinery Design (TMD) code is developed by the KAIST research team written in MATLAB environment. It can estimate the performance and geometry of turbines at the design point and the performance at various off-design points. The design method of KAIST-TMD code is briefly described in this paper and more detail can be found in [5].

Mass conservation (2) and Euler equations (3) are used for the design of turbomachineries based on 1-D mean line analysis because both equations can be applied regardless of the real or ideal gas.

$$\dot{m} = \rho(h_{st}, P_{st})AV \qquad (2)$$

$$\Delta h_{turbine} = h_{o2} - h_{o1} = U_2 V_{\theta 2} - U_1 V_{\theta 1} \qquad (3)$$

However, since all of the work of the turbomachinery is not produced in an isentropic process, losses have to be considered. Losses measure how far the actual process is from the ideal isentropic process. These losses can be defined with pressure loss or enthalpy loss as shown in Fig. 5. A literature review has shown that pressure loss models can be easily applied to axial turbomachineries and enthalpy loss models can be applied to radial turbomachineries [12, 13]. Therefore, in KAIST-TMD, the pressure loss models are applied to the axial turbine and compressor, and the enthalpy loss models are used for the radial turbine and compressor design and analyses.

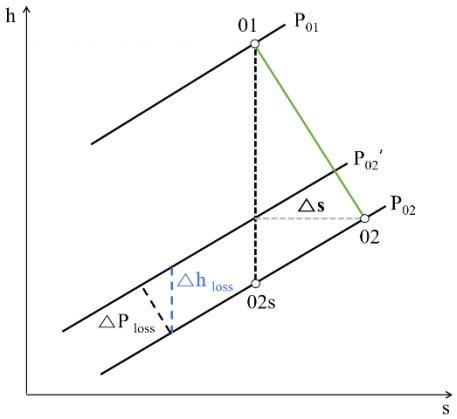

Fig. 5. h-s diagram of enthalpy and pressure loss model

Table.2 Summary of the loss model of each turbomachineries

Axial turbine	
Profile loss	Balje-Binsley [14]
Secondary loss	Kacker-Okaapu [15]
Tip clearance loss	Dunham-Came [16]
Radial compressor	
Incidence loss	Boyce [17]
Blade loading loss	Coppage et al. [18]
Skin friction loss	Jansen [19]
Clearance loss	Jansen [19]
Disk friction loss	Daily and Nece [20]
Mixing loss	Johnston and Dean [21]
Recirculation loss	Oh et al. [13]
Leakage loss	Aungier [22]
Radial turbine	
Incidence loss	Balje [23]
Rotor passage loss	Balje [23]
Clearance loss	Jansen [19]
Disk friction loss	Daily and Nece [20]

Using the models summarized above, a turbomachinery design in-house code, KAIST-TMD, was developed which is again written in MATLAB. The main code structure is shown in Fig. 6.

The main design variables are defined by the designer when designing the turbine with KAIST-TMD. Then the off-design values and the geometry values are calculated through the iteration process with the selected loss models suitable for the

 DOI: 10.17185/duepublico/48896

selected turbomachinery. The property values are referred from REFPROP developed by National Institute of Standards and Technology (NIST) [11].

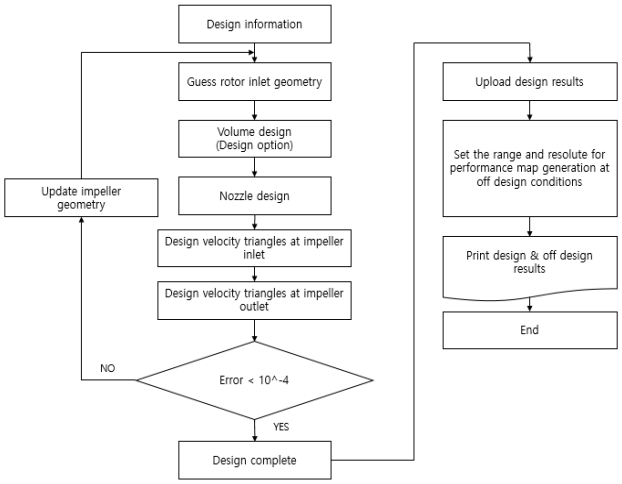

Fig. 6. Main algorithm of KAIST-TMD [5]

KAIST-HXD

The KAIST Heat eXchanger Design (HXD) code is based on MATLAB environment and was developed to design a printed circuit heat exchanger (PCHE) for the S-CO_2 power system applications. To overcome dramatic changes of properties of CO_2 near the critical point, the discretized design and analysis method is adopted in place of widely used conventional heat exchanger design methods such as LMTD method. In KAIST-HXD, the energy and momentum governing equations are solved numerically to calculate properties of CO_2 in finite number of volumes [6]. It performs analysis on the unit channel representing the entire heat exchanger. The total heat transfer for one control volume is calculated as follows.

$$Q = UA\Delta T = \frac{1}{\frac{1}{h'_{hot}A}+\frac{t}{h'_{conduction}A}+\frac{1}{h'_{cold}A}}\ \Delta T \qquad (4)$$

To obtain pressure drop for one control volume, the friction factor must be determined. Friction pressure drop equation is as follows:

$$\Delta P = f\frac{l}{D_e}\frac{\rho V^2}{2} \qquad (5)$$

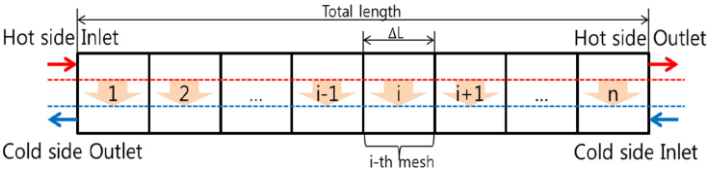

Fig. 7. Channel nodalization in KAIST_HXD [6]

Using the above equations, the inlet and outlet temperatures and pressures for one channel can be determined by the enthalpy change due to heat transfer and the pressure drop due to friction. The cold side can be calculated as above, but since the flow direction of the hot side is opposite to that of the cold flow (i. e. counter current), the calculation starts from the outlet of the cold side to the inlet. Therefore, the property of the cold side outlet should be assumed first. If the cold side inlet result obtained from the assumed cold outlet does not satisfy the cold inlet temperature calculated in the heat transfer equation and pressure boundary conditions, the new cold outlet temperature and pressure are assumed and the calculation is conducted again until the convergence conditions are met.

MOTIVATION OF AXIAL TURBINE DESIGNED UNDER THE CONDITION OF KAIST-MMR

The original MMR is designed to have an output of 12MWe, and the type of turbine satisfying these conditions is shown in Fig. 8 [24], which shows that both radial type turbine and axial turbine can be appropriate. In the previous MMR design, the design choice was using a single stage radial turbine.

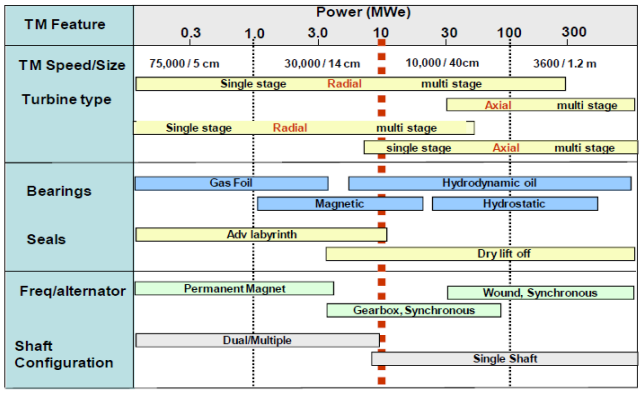

Fig. 8. Component and technology options for S-CO_2 cycles [24]

The existing MMR radial turbine was designed at the boundary between the radial turbine and the axial turbine as shown in Fig. 8. In other words, it is designed to have the maximum capacity that can be covered by the single stage of radial turbine. If the capacity of the existing MMR becomes larger, the number of stages for the radial turbine has to increase or using axial turbine can be another choice. However, in the case of radial turbine, it is not recommended to increase the number of stages because the inter-stage flow path can induce large pressure drop, so an axial turbine can be more appropriate [25]. Before designing an axial turbine for the larger MMR, it is possible to evaluate the performance of an axial turbine compared to a radial turbine for existing MMR.

 DOI: 10.17185/duepublico/48896

Therefore, the purpose of this paper is summarized as the following: 1. Design an axial turbine suitable for MMR. 2. Evaluate the potential for using an axial turbine for MMR by comparing off design performance with originally designed single stage radial turbine. The design is performed by using KAIST CCD and TMD codes. For the isolated grid application, timely transient response is imperative, therefore the newly designed MMR was evaluated with GAMMA + code and compared to the radial turbine based on MMR.

COMPARISON OF RADIAL AND AXIAL TURBINES

An axial turbine was designed to replace a radial turbine under the conditions of original MMR using KAIST-TMD code described above. Using the KAIST-TMD code, the following results were obtained.

A turbomachinery map was generated for the range of possible mass flow rates by raising the rpm from 60% to 120% of the design point for performance evaluation. The range of possible mass flow rates depends on the rpm. The minimum possible mass flow rate is 24% of the design point at rpm = 11,580 and the maximum possible mass flow rate is 126% of the design point at rpm = 17,370.

Table 3. The range of performance evaluation and design point of turbine

The range of the mass flow rate (min to max)	24-126%
The range of the rpm	60-120%
The rpm of design point	19300
The mass flow rate of design point	180kg/s

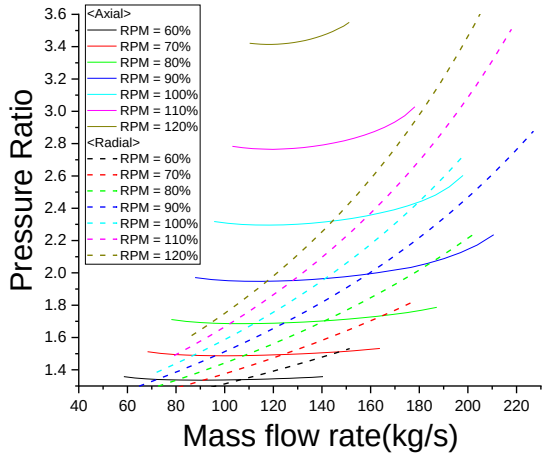

Fig. 9. Comparison of Pressure ratio map for MMR radial and axial turbines

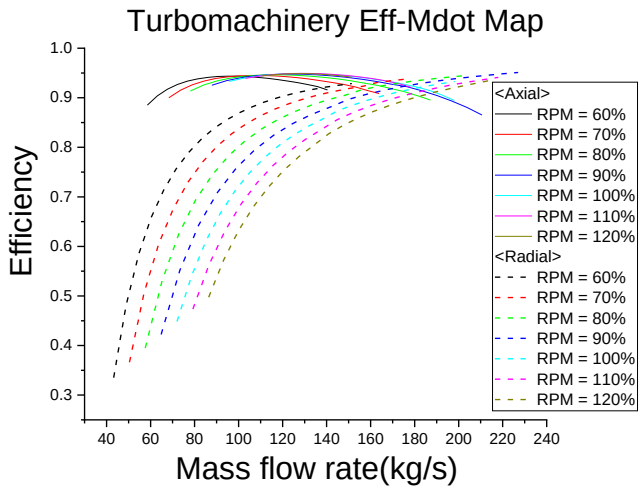

Fig. 10. Comparison of efficiency map for MMR radial and axial turbines

Figs. 9 and 10 show the pressure ratio-mass flow rate map and the efficiency-mass flow rate map of the axial turbine and the radial turbine. Results are generated from KAIST-TMD code. The performance map shown in Figs. 9 and 10 show that the slope is smooth compared to the radial turbine in both pressure ratio and efficiency for the axial turbine when the mass flow rate deviates from the design point. On the other hand, under the same conditions, the radial turbine shows a rapid change in efficiency and pressure ratio, which means that the axial turbine can operate in more stable performance than the radial under the off design operating conditions. In order to analyze these results, loss of radial turbine and axial turbine of KAIST-TMD code were obtained respectively.

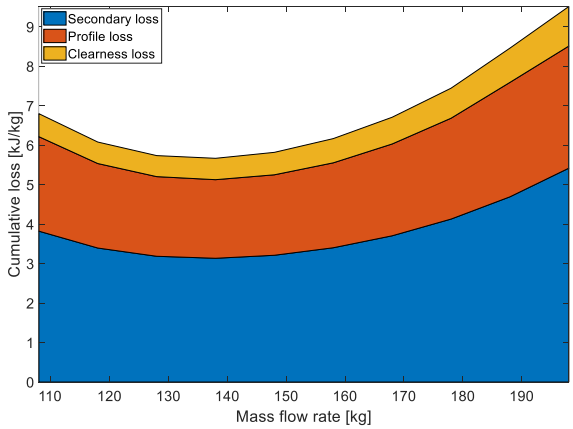

Fig. 11. The cumulative loss of the axial turbine – mass flow rate graph

 DOI: 10.17185/duepublico/48896

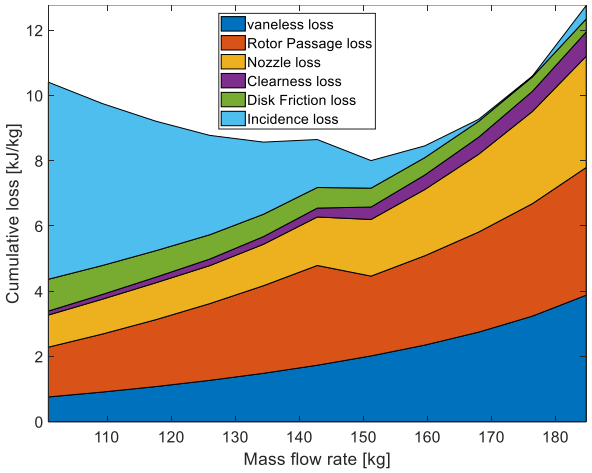

Fig. 12. The cumulative loss of the radial turbine – mass flow rate graph

The losses of radial turbine and axial turbine of KAIST TMD code were obtained as follows. Comparing Figs. 11 and 12, the overall cumulative loss for axial turbine is smaller than that of the radial turbines. Because the incidence loss for radial turbine which is generated during the off-design condition due to the mismatch of the direction of relative velocity of fluid at inlet and inlet blade angle is larger than that of the axial turbine. In addition, the incidence loss decreases with the approach to the design point, but since the vaneless space loss which occurs in a vaneless space between the impeller vane and the diffuser vane becomes larger as the mass flow rate increases, the efficiency of the radial turbine is higher than that of the radial turbine in the wide-range of off-design condition.

Therefore, these results show that the axial turbine has potentially better performance than the radial turbine under the off-design operation, and it is a motive to evaluate the potential of MMR using an axial turbine. As a result, the following design values were obtained and shown in Table 4.

Table 4. TMD code result of axial turbine MMR cycle

Number of stages	8
Turbomachinery work	21.53MW
Total-to-total-Pressure Ratio	2.44
Total-to-total efficiency	91.57%

Using the above results, the cycle was optimized by using KAIST-CCD code. It should be noted that the axial turbine for MMR developed conceptually in this paper is designed to be similar to the CSP turbine which is four stages axial turbine used in the Sunshot project. The developed turbine is for 10 MW power output CSP solution [26].

The CSP turbine was developed by aero design tools and full scale CFD tool was also used. A 4-stage design with 27000 RPM is selected due to the reduction of mechanical stress and the improvement of efficiency as shown in Fig. 13.

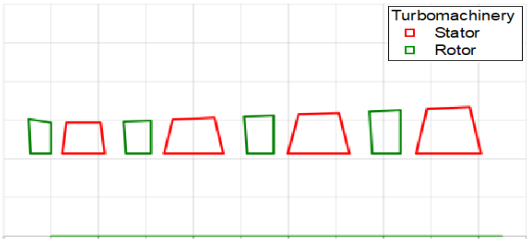

Fig. 13. Preliminary flow path layout of the 4-stage axial turbine [26]

Although it is designed with similar concepts, the CSP turbine produces 10 MW_e of power output with 27,000 rpm, four stages, while the axial turbine designed in this paper produces 12MW of power output with 19,300 rpm, 8 stages. From the viewpoint of the number of stages, it seems reasonable that the CSP turbine has better performance than the axial turbine designed in this paper. However, the CSP turbine has an rpm of 27,000, while the MMR axial turbine developed in this paper has an rpm of 19,300 due to the synchronized compressor. Therefore, if the rpm is increased to about 27,000, a turbine with four stage having similar performance can be produced by using KAIST_TMD code. This is left as future works for the further design optimization of the MMR.

OPTIMIZATION OF CYCLE FOR MAXIMIZING EFFICIENCY

In this paper, MMR using axial turbine was optimized under the original MMR condition by KAIST-CCD for selecting the highest efficiency. In other words, in case of MMR using axial turbine, the efficiency and pressure ratio of the turbine are changed from the input values of the original MMR using radial turbine and used as input values in the KAIST CCD code. The new input values of MMR using axial turbine are as follows.

Table 5. The input values of MMR using axial turbine for KAIST CCD

Thermal power	36.2MW_{th}	Cycle layout	Simple brayton recuperation
Mechanical efficiency	98%	Total-to-total Pressure ratio	2.44
Turbine total-to-total efficiency	91.57%	Compressor total to total efficiency	85%
Generator efficiency	98%	Rotating speed	19,300rpm
Max Pressure	20Mpa	Recuperator effectiveness	95%
Max Temperature (Turbine inlet)	550 ℃	Min Temperature (Compressor inlet)	60 ℃

 DOI: 10.17185/duepublico/48896

The T-S diagram obtained from the KAIST-CCD code and the property values such as temperature and pressure are shown in Table 6. T-S diagrams for new MMR with an axial turbine are shown in Fig. 14 to compare with the thermodynamic property values of original MMR with the radial turbine. The numbers in Fig. 14 correspond to the node numbers in MMR shown in Fig. 4, respectively.

Table 6. The optimization design value of new MMR using axial turbine

Mass Flow rate		182.15kg/s
Point	Temperature(°C)	Pressure(Mpa)
1	550	19.93
2	440.72	8.17
3	156.47	8.10
4	60	8.01
5	141.96	20
6	388.48	19.98
7	550	19.93

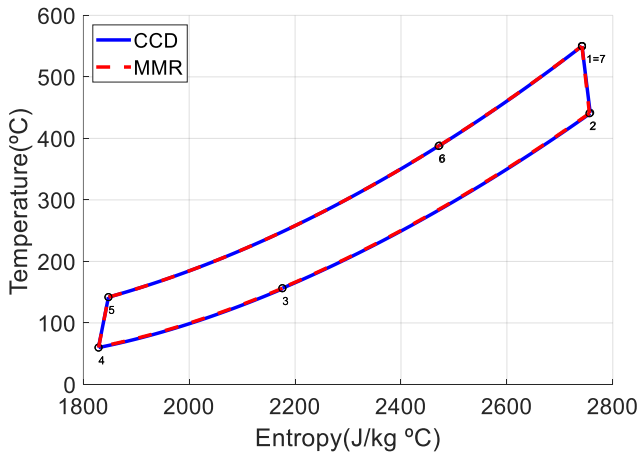

Fig 14. Comparison of T-s diagram of MMR and result of CCD code

As a result, it was confirmed that there is almost no difference in properties between two MMRs. This means that there is almost no difference in the T-s diagram between the cycle using the axial turbine with the best efficiency and that of the radial turbine. Therefore, since the GAMMA + code of original MMR using radial turbine is already constructed, only the turbine will be modified in the GAMMA+ transient simulation.

The KAIST research team modified GAMMA + code to become applicable to the original MMR. GAMMA+ code is originally developed for a gas cooled reactor transient analysis by KAERI. However the original GAMMA + code is designed to calculate the CO_2 properties with simple correlation, but it was necessary to calculate the CO_2 property values near the critical point more accurately. The modified GAMMA + code used the REFRPOP program developed by NIST to solve the above problems [11]. The REFRPOP program accurately calculates the thermal and transport properties of various fluids, including CO_2. The modified GAMMA + code with NIST database for CO_2 properties near the critical point was validated using experimental data from SCO2PE [27].

As mentioned above, since the results obtained by using KAIST CCD code and the original value of MMR show no marked changes, GAMMA+ code of MMR can be adopted identically except for the turbine section, which are replaced by newly formed axial turbines. The design points under steady state of the main part of the cycle obtained by GAMMA + code is shown in Fig. 15.

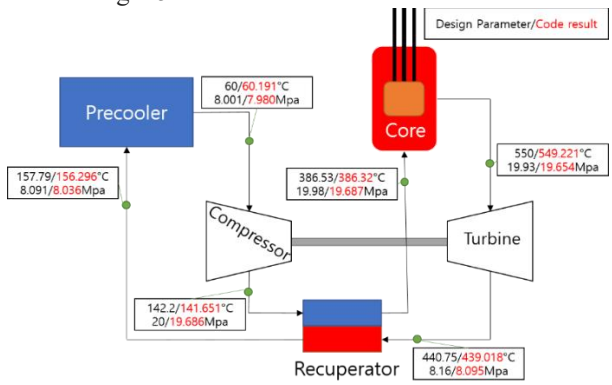

Fig 15. Comparison of design parameters and code result in the main part of the cycle

As shown in Fig. 15, the results of the code also show no dramatic changes compared to the original design points, but a slight difference of 0-0.3MPa occurs for the pressure. This seems to be due to the more precise consideration of the pressure drop using the Blasius ($Re < 30000$) & McAdams ($30000 < Re < 10^6$) correlations for pipe and Baik's correlation [6] for PCHE in GAMMA+ code, while KAIST_CCD does not accurately account for the pressure drop.

To compare the dynamic performance of the new MMR with the axial turbine and the original MMR with the radial turbine, it is assumed that a scenario simulating the load change and it is prescribed by MMR. The load varied from 100% to 70% and then back to 100%. This scenario starts at steady state (t = 100 s), during which the load drops from 100% to 70% (t = 100-300s) for 200 seconds and rises from 70% to 100% for another 200 seconds (t = 400-600 seconds).

The results using both radial and axial turbines applied to the MMR system are shown Figs. 16 to 25. The load changed to the scenario mentioned above, and the result is shown in Fig. 16.

 DOI: 10.17185/duepublico/48896

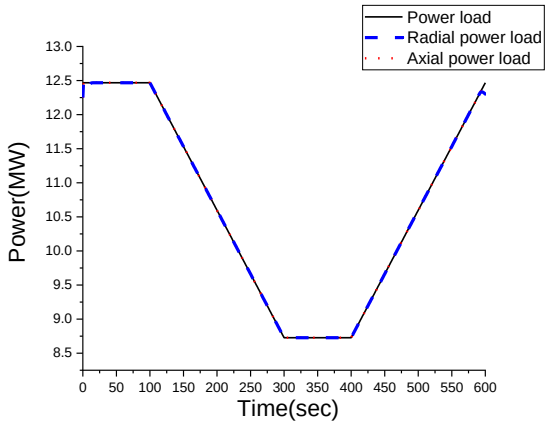

Fig. 16. Load of MMRs with Radial and Axial turbines

The results of the transient analysis show that thermal power of the MMR with an axial turbine are similar to those of the MMR with radial turbine as shown in Fig. 16, and the cycle efficiency of MMR with axial turbine comparable to the MMR with radial turbine in the off-design point in Fig. 18.

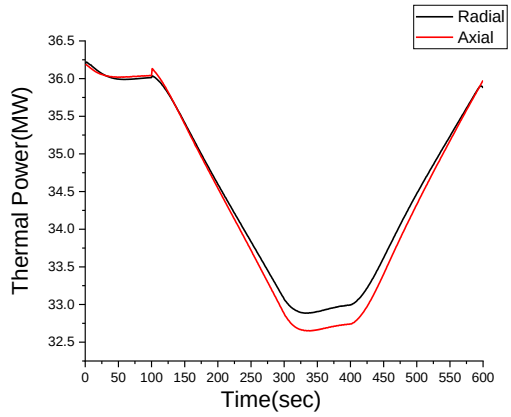

Fig. 17. Thermal power of MMR of Radial and Axial turbines

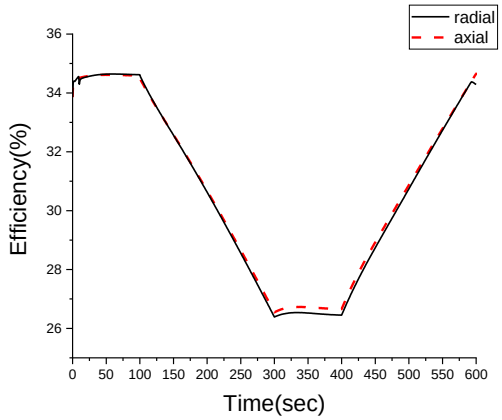

Fig. 18. Efficiency of MMRs with Radial and Axial turbines

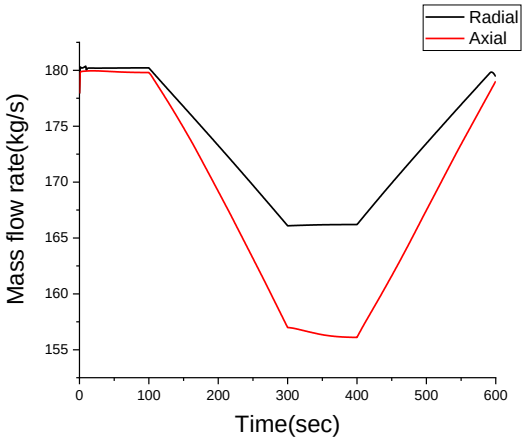

Fig. 19. Mass flow rate of MMRs with Radial and Axial turbines

Displayed from the efficiency maps of radial turbine and axial turbine in Fig. 10, the efficiency graphs of the axial turbine remain unchanged from the design efficiencies, whereas the graphs of the radial turbine drop abruptly as the mass flow rate decreases as shown in Fig. 19.

In Fig. 20, it can be seen that there is almost no difference between the radial and axial turbine works. This is because the same radial compressor was used and the thermal power and efficiency in axial and radial cases are similar, as shown in Figs. 16 and 17.

$$\dot{W}_{t,turbine} = \dot{Q}_{core}\eta_{thermal} + \dot{W}_{t,compressor} \qquad (6)$$

Where $\dot{W}_{t,turbine}$ = Turbine work, $\dot{W}_{t,compressor}$ = Compressor work, $\dot{Q}_{core}$=Thermal power of MMR, η_{thermal} = thermal efficiency of cycle.

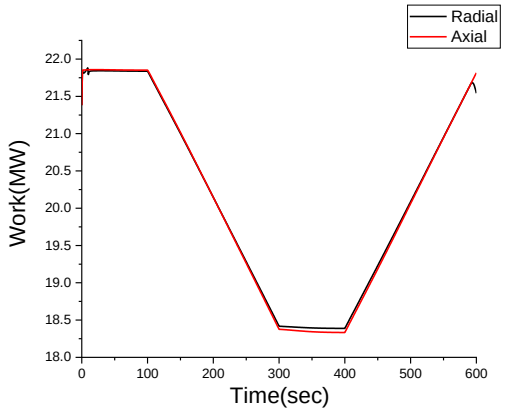

Fig. 20. Turbine work of MMRs with Radial and Axial turbines

The radial and axial turbine works are similar, but the mass flow

rate is relatively different. Therefore, the relationship between turbine work and mass flow rate has to be considered.

The formula for turbine work is:

$$\dot{W}_{t,turbine} = \dot{m}\Delta h_{turbine} \qquad (7)$$

Where $\Delta h_{Turbine} = = h_{o2} - h_{o1} = U_2 V_{\theta 2} - U_1 V_{\theta 1}$, Enthalpy difference between the turbine inlet and outlet

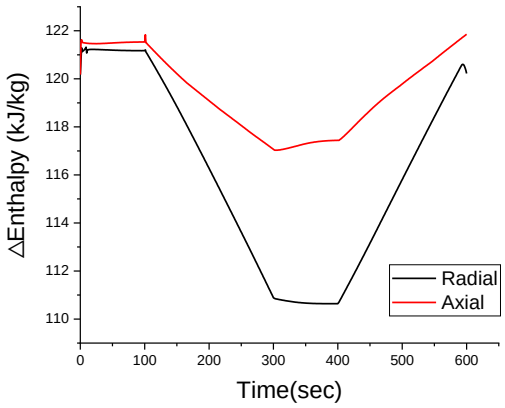

Fig. 21. Enthalpy change between the turbine inlet and outlet of MMR of Radial and Axial turbines

At the off-design point, the enthalpy difference ($\Delta h_{Turbine}$) of the MMR with axial turbine is larger than that of the MMR with radial turbine as shown in Fig. 21 because the mass flow rate ($\dot{m}$) of the axial turbine is relatively reduced and turbine work of the axial and radial is no difference.

The implications of the results show the advantages of using the axial turbine over the radial turbine. Although the axial turbine operates at comparable efficiencies to radial turbine for off-design ranges, it retains its high $\Delta h_{turbine}$ compared to the radial turbine which consequently leads to having lower mass flow rate under a given turbine work. As a result, the specific work of the turbine is increased at lower load conditions when the axial turbine is adopted as shown in Fig. 21. The advantage will be amplified as the system capacity increases, and thus, the axial turbine will prove beneficial for larger size systems.

SUMMARY AND FUTURE WORKS

In this paper, an axial turbine was designed to replace the radial turbine of the KAIST MMR and the transition analysis was performed.

First, axial turbine was designed with KAIST_TMD code by using MMR design conditions for radial turbine system (turbine inlet temperature and pressure, turbine outlet pressure, rpm, mass flowrate) developed by KAIST research team. As a result, an axial turbine with eight stages was designed which has a turbine work of 21.53 MW, a pressure ratio of 2.44, and a turbine efficiency of 91.57%.

Second, an optimization was performed with KAIST_CCD code using the newly designed system with axial turbine. As a result, the T-s diagram shows that there is almost no difference between the properties of the original MMR and the new MMR. Therefore, the code for performing the transition analysis with GAMMA + code was created by using the operating conditions of the existing MMR, except for the newly developed axial turbine.

Third, in order to perform the transient analysis of MMR with axial turbine, GAMMA + code is implemented at the scenario where load is changed from 100%-70%-100%. As a result, it was found that the efficiency of the MMR with axial turbine is comparable to the near design point and wider operating range of MMR is possible with axial turbine. Furthermore, axial turbine shows high specific work compared to the radial turbine which leads to having lower mass flow rate for the given turbine work. As a result, the specific work by the turbine can be increased at lowered load conditions when the axial turbine is adopted in the system.

In this study, the potential of the axial turbine was confirmed in terms of specific work under the off-design conditions when axial turbine or radial turbine is used. The axial turbine is more advantageous with respect to the specific work compared to the radial turbine under off-design conditions and these advantages will be amplified as the system becomes large. In addition, when the new system is bigger than the system of MMR, the advantages of axial turbine is maximized because axial turbine has better efficiency than the radial turbine for larger system.

Finally, the planned future works are to design the MMR with 4-stage axial turbine to operate at higher efficiency.

NOMENCLATURE

A	Surface area of the heat transfer [m^2]
A′	Flow area [m^2]
D	Diameter [m]
D_e	Equivalent diameter [m]
K	Form loss
P	Pressure [Pa]
Q	Thermal power [W]
R	Chemical reaction
T	Temperature [K]
U	Impeller tip speed [m/s]
V	Flow velocity [m/s]
Y	Mass fraction
W	Relative velocity [m/s]
W_t	Specific work [W/kg]
f	Friction factor

 DOI: 10.17185/duepublico/48896

g	Gravitational acceleration $[m/s^2]$
h	Enthalpy [J/kg]
h′	Heat transfer coefficient $[W/m^2K]$
ṁ	Mass flow rate [kg/s]
q	Specific heat [J/kg]
q′′	Heat flux $[W/m^2]$
j	Diffusion flux $[mol/m^2s]$
t	Time [sec]
z	Height [m]
ρ	Density $[kg/m^3]$

Subscript

o	Stagnation condition
s	Species
st	Static condition

REFERENCE

[1] Steven A. Wright, Ross F. Radel, Milton E. Vernon, Gary, E. Rochau, Paul S. Pickard, "Operation and Analysis of a Supercritical CO_2 Brayton Cycle, Sandia National Laboratories, Sandia Report", SAND2010-0171.

[2] White, C., "Analysis of Brayton Cycles Utilizing Supercritical Carbon Dioxide," National Energy Technology Laboratory, DOE/NETL-4001/070114 (2014).

[3] S. G. Kim, et al., Conceptual System Design of a Supercritical CO_2 cooled Micro Modular Reactor, Proceedings of ICAPP, 2015.

[4] M.S.Kim, Y.H.Ahn, B.J.Kim, J.I.Lee, "Study on the supercritical CO_2 power cycles for landfill gas firing gas turbine bottoming cycle.", Energy, 111(2016), pp. 893-909

[5] J.K. Lee, J.I. Lee, Y.H. Ahn and H.J. Y, Design methodology of supercritical CO_2 brayton cycle turbomachineries, ASME Turboexpo, Copenhagen, Denmark, 2012

[6] Seungjoon Baik, Seong Gu Kim, Jekyoun Lee, Jeong Ik Lee, "Study on CO_2-water printed circuit heat exchanger performance operating under various CO_2 phases for S-CO_2 power cycle application", Applied Thermal Engineering, 2017.

[7] Kofskey, Milton G., and Donald E. Holeski. Cold performance evaluation of a 6.02-inch radial inflow turbine designed for a 10-kilowatt shaft output brayton cycle space power generation system. Vol. 2987. National Aeronautics and Space Administration, 1966

[8] S.K.Cho. "Study on supercritical CO_2 radial turbine design methodology for decay heat removal system of sodium cooled fast reactor." (2016).

[9] J.H.Kim. "A Review of Helium Gas Turbine Technology for High-temperature Gas-cooled Reactors". Nuclear Engineering and Technology, v. 39. no. 1, pp.21-30(2007)

[10] Takizuka, Takakazu, et al. "R&D on the power conversion system for gas turbine high temperature reactors." Nuclear Engineering and Design 233.1-3 (2004): 329-346.

[11] E.W. Lemmon, M.L. Huber, and M.O. McLinden, "NIST Standard Reference Database 23," NIST Reference Fluid Thermodynamic and Transport Properties –REFPROP, version, vol.9, p.55, 2010.

[12] Ji Hwan Kim, Hee Cheon No. A Gas Turbine Code for Off-Design Performance and Transient Analysis of High-Temperature Gas-Cooled Reactors, 2008.

[13] Hyoung Woo Oh, Myung Kyoon Chung. Investigation on the Design and Performance Analysis Methods of Centrifugal Turbomachines, 1998.

[14] O.E. Balje and R.L. Binsley, Axial turbine Performance Evaluation. Part A - Loss-Geometry Relationship, Journal of Engineering for Power, Transactions of the ASME, pp. 341-348, 1968.

[15] S.C. Kacker and U. Okapuu, A Mean Line Prediction Method for Axial Flow Turbine Efficiency, Journal of Engineering for Power, Transactions of the ASME, Vol. 104, pp. 111-119,1982.

[16] Dunham, J., and P. M. Came. "Improvements to the Ainley-Mathieson method of turbine performance prediction." Journal of Engineering for Power 92.3 (1970): 252-256.

[17] Boyce, Meherwan P, Centrifugal compressors : a basic guide, PennWell, 2003

[18] Coppage, J. E., Dallenbach, F., Eichenberger, H. P.,Hlavaka, G. E., Knoernschild, E. M. and Van Lee, N. Study of supersonic radial compressors for refrigeration and pressurization systems, WADC Report 55-257, 1956.

[19] Jansen, W. A method for calculating the flow in a centrifugal impeller when entropy gradients are present, Royal Society Conference on Internal Aerodynamics (Turbomachinery),1967 (IME).

[20] Daily, J. W. and Nece, R. E. Chamber dimension effects on induced flow and frictional resistance of enclosed rotating disks, Transactions of the ASME, J. Basic Engng, Vol. 82, pp.217-232, 1960.

[21] Johnston, J. P. and Dean Jr, R. C. Losses in vaneless diffusers of centrifugal compressors and pumps. Analysis, experiment,and design, Transactions of the ASME, J. Engine for Power, Vol. 88, pp. 49-62, 1966.

[22] Aungier, R. H., Mean streamline aerodynamic performance analysis of centrifugal compressors, Transactions of the ASME, J. Turbomachinery, Vol. 117, pp. 360-366, 1995.

[23] Balje, O. E., A Contribution to the Problem of Designing Radial Turbomachines, Transactions of the ASME, Vol. 74,pp. 451, 1952

[24] Sienicki James J., Anton Moisseytsev, Robert L. Fuller, Steven A. Wright and Paul S. Pickard, "Scale Dependencies of Supercritical Carbon Dioxide Brayton Cycle Technologies and the Optimal Size for a Next-Step Supercritical CO_2 Cycle Demonstration", SCO_2 Power Cycle Symposium, 2011.

[25] Philip P. Walsh, Paul Fletcher, "Gas Turbine Performance", Second Edition, pg 206- 215, 2004.

[26] Chiranjeev Kalra, et al., Development of high Efficiency hot gas turbo-expander for optimized CSP supercritical CO_2 power block operation, The 4th International Symposium - Supercritical CO_2 Power Cycles

[27] Bae, Seong Jun, et al. "Comparison of gas system analysis code GAMMA+ to S-CO_2 compressor test data." ASME Turbo Expo 2015: Turbine Technical Conference and Exposition. American Society of Mechanical Engineers, 2015.

DOI: 10.17185/duepublico/48896
URN: urn:nbn:de:hbz:464-20191004-111651-2